

# UNIVERSITY OF BIRMINGHAM

## Research at Birmingham

### Beautiful clusters - Boron-9

Kokalova, Tz; Wheldon, Carl

*DOI:*

[10.1088/1742-6596/863/1/012023](https://doi.org/10.1088/1742-6596/863/1/012023)

*License:*

Creative Commons: Attribution (CC BY)

*Document Version*

Publisher's PDF, also known as Version of record

*Citation for published version (Harvard):*

Kokalova Wheldon, T & Wheldon, C 2017, 'Beautiful clusters - Boron-9: Simulations and decay', *Journal of Physics: Conference Series*, vol. 863, no. 1, 012023. <https://doi.org/10.1088/1742-6596/863/1/012023>

[Link to publication on Research at Birmingham portal](#)

**Publisher Rights Statement:**

Checked for eligibility: 31/07/2017

**General rights**

Unless a licence is specified above, all rights (including copyright and moral rights) in this document are retained by the authors and/or the copyright holders. The express permission of the copyright holder must be obtained for any use of this material other than for purposes permitted by law.

- Users may freely distribute the URL that is used to identify this publication.
- Users may download and/or print one copy of the publication from the University of Birmingham research portal for the purpose of private study or non-commercial research.
- User may use extracts from the document in line with the concept of 'fair dealing' under the Copyright, Designs and Patents Act 1988 (?)
- Users may not further distribute the material nor use it for the purposes of commercial gain.

Where a licence is displayed above, please note the terms and conditions of the licence govern your use of this document.

When citing, please reference the published version.

**Take down policy**

While the University of Birmingham exercises care and attention in making items available there are rare occasions when an item has been uploaded in error or has been deemed to be commercially or otherwise sensitive.

If you believe that this is the case for this document, please contact [UBIRA@lists.bham.ac.uk](mailto:UBIRA@lists.bham.ac.uk) providing details and we will remove access to the work immediately and investigate.

## Beautiful clusters – boron-9: simulations and decay

This content has been downloaded from IOPscience. Please scroll down to see the full text.

2017 J. Phys.: Conf. Ser. 863 012023

(<http://iopscience.iop.org/1742-6596/863/1/012023>)

View [the table of contents for this issue](#), or go to the [journal homepage](#) for more

Download details:

IP Address: 147.188.254.76

This content was downloaded on 12/07/2017 at 17:15

Please note that [terms and conditions apply](#).

You may also be interested in:

[High-resolution particle spectroscopy of  \$^{186}\text{Re}\$](#)

C Wheldon, N I Ashwood, N Curtis et al.

[A Search for Capture Processes in Alpha-Particle and Deuteron Bombardments](#)

H R Allan and N Sarma

[Methods and progress in studying inelastic interactions between positrons and atoms](#)

R D DuBois

[Dynamics of Dark and Visible Matter in Galaxies: Simulations and Observations](#)

Stephen G. Vine

[Positron emission tomography](#)

Hans Lundqvist, Mark Lubberink and Vladimir Tolmachev

# Beautiful clusters – boron-9: simulations and decay

Tz Kokalova Wheldon and C Wheldon

School of Physics and Astronomy, University of Birmingham, Edgbaston, Birmingham  
B15 2TT, UK

E-mail: [t.wheldon@bham.ac.uk](mailto:t.wheldon@bham.ac.uk)

**Abstract.** Monte-Carlo simulations for analysis of the  ${}^9\text{Be}({}^3\text{He}, t){}^9\text{B}^*$  reaction at 33 MeV using coincidences between the high-resolution Munich Q3D spectrograph and the large-acceptance Birmingham silicon detector array are presented. These focus on the identification of the proton break-up product and the application to evidencing the first excited  $1/2^+$  state. Identifying this state has posed a challenge for over 70 years, but would enable the mirror symmetry in this light system to be explored, giving insight into its possible clustered structure. Penetrabilities for the low excitation energy regime are calculated showing the efficacy of the proton-identification method.

## 1. Introduction

The unstable isotope,  ${}^9\text{B}$  has a half-life of approximately  $6 \times 10^{-19}$  s ( $\Gamma = 0.54 \pm 0.21$  keV [1]) and was first discovered in 1940 by Haxby and coworkers [2, 3]. What is particularly interesting about  ${}^9_5\text{B}_4$  is the comparison with its mirror partner  ${}^9_4\text{Be}_5$ . The first excited state in  ${}^9\text{Be}$  lies at 1.684(7) MeV with  $I^\pi = 1/2^+$  [1] yet, notably, in  ${}^9\text{B}$ , this state has not been firmly established. There have been many experimental studies over the last 70+ years, reporting the state anywhere from 0.8-1.9 MeV [4] and this activity has been matched by theoretical calculations with a similar energy spread [5, 6, 7]. Solving this persistent mystery is so important due to its relevance to understanding the structure of both the  ${}^9\text{B}$  and  ${}^9\text{Be}$  states and precision tests of the nuclear force. There are two possible structures for the  $I^\pi = 1/2^+$  resonances, either a compact shell-model configuration of core-plus-valence-nucleon, or a more extended nuclear molecular arrangement in which a covalent nucleon binds the two  $\alpha$ -particle clusters. Measuring the Coulomb energy difference (CED) between the two mirror  $I^\pi = 1/2^+$  states enables, through its sensitivity to the volume, the structure to be established – the clustered state being the larger of the two.

There are several reasons why the state has been difficult to establish in  ${}^9\text{B}$ . Firstly, in most reactions, the population of any  $I^\pi = 1/2^+$  strength is weak. Secondly, the proximity of levels such as the  $I^\pi = 5/2^-$  level ( $\Gamma = 81(5)$  keV) at 2.361(5) MeV, the 2.75(30) MeV  $I^\pi = 1/2^-$  state ( $\Gamma = 3.1(2)$  MeV) and the 2.79(3) MeV  $I^\pi = 5/2^+$  level ( $\Gamma = 550(40)$  keV) [1] mean there is significant background obscuring any  $I^\pi = 1/2^+$  signal. For some of these the decay mode can be utilised, with coincidence methods, to suppress states. For example the proton channel is open for all states ( $S_p = -0.186$ ) MeV, but the  $\alpha$  threshold lies at 1.687 MeV. For this reason the ‘missing’  $I^\pi = 1/2^+$  resonance is expected to decay predominantly via proton emission and this can be separated from the 2.36 MeV state which decays 99% through the  $\alpha$  channel [8, 9]. This is necessary due to the strong population of this and higher-lying levels. The present authors were involved in a recent study that used the Munich Q3D spectrograph [10, 11, 12] in coincidence

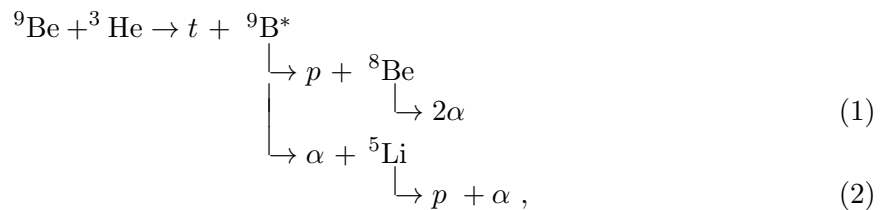


with the Birmingham large area double-sided silicon strip detector (DSSD) array to study the  ${}^9\text{Be}({}^3\text{He}, t){}^9\text{B}^*$  reaction at 33 MeV, recording both the ejectile (with high resolution at the Q3D focal plane) and break-up products (in the DSSD array). That work [8] reported a state at 1.86 MeV  $\pm 70$  keV(stat)  $\pm 35$  keV(syst) and  $\Gamma = 650 \pm 160$  keV, in close agreement with two other studies using the same reaction without coincidences and at significantly higher beam energies: 1.80 $^{+0.22}_{-0.16}$  MeV with  $\Gamma = 600^{+300}_{-270}$  keV [13] and 1.850 $\pm 0.130$  MeV with  $\Gamma = 700^{+270}_{-200}$  keV [14]. The difference in Ref. [8] was that, due to the coincidence-filtering, the state observed was isolated and formed a visible feature in the spectrum.

This paper reports details of the Monte-Carlo simulations carried out to aid the analysis of Ref. [8] and also discusses the anomalous decay of the 2.36 MeV state. Details of the experimental set-up and other aspects of the analysis are given in Ref. [8].

## 2. Simulations

The program RESOLUTION8 [15, 16], developed by the Birmingham group, was used to generate events for the following two break-up reactions:



(2)

each having an overall  $Q$ -value of  $-0.809$  MeV. In order to speed up the simulation, events were only generated for which the triton laboratory angle lay within the acceptance of the Q3D spectrograph (slits set to  $\theta_{\text{in-plane}} = \pm 1.43^\circ$  and  $\theta_{\text{out-of-plane}} = \pm 2.0^\circ$ ) before smearing. This facilitated the production of  $10^6$  events within  $\sim 10$  min.

The effects included in the simulation were,

- initial two-body reaction with  $Q = -1.087$  MeV and a uniform centre-of-mass distribution across the Q3D acceptance;
- entire energy range of the focal-plane; 0.480-2.700 MeV generated;
- the break-up of the  ${}^9\text{B}$  recoil into either  ${}^8\text{Be}+p$  ( $Q = 0.186$  MeV) or  ${}^5\text{Li}+\alpha$  ( $Q = -1.687$  MeV) for which a uniform distribution in spherical polar angles was generated randomly per event;
- break-up of the heavy fragment into  $2\alpha$  ( $Q = 0.092$  MeV) or  $\alpha+p$  ( $Q = 1.965$  MeV);
- Smearing of the  ${}^5\text{Li}$  ground-state was added to the second stage of break-up (2) via a random Gaussian energy distribution centred at  $E_x({}^5\text{Li}) = 0$  MeV with a FWHM equal to the width of the  ${}^5\text{Li}$  ground-state,  $\Gamma = 1.23$  MeV [17];
- beam divergence and finite beam-spot size;
- energy loss and energy and angular straggling in the target;

These events were analysed with the code used for the experimental data following some preprocessing. Initially, the in- and out-of-plane angles for each detector strip were calculated so that the energy and position information of each particle making up the simulated events could be transformed into strip/ADC number. This enabled the appropriate channel-by-channel thresholds to be set and dead-strips to be removed. Additionally, the particles incident on the silicon array had their energies smeared to give a front-back energy distribution that matched the experimental data. For the triton events, the centre angle of the Q3D was taken, in this case,  $30^\circ$ . This had one of the largest smearing effects on the final kinematic reconstruction of

the data. All other processing was done with energy-ordered silicon data, just as for the real data and the reconstructions were done using the same processing code, *i.e.* without knowledge of the particle type for hits in the DSSD array.

In order to cleanly select events, part of the analysis procedure required a proton gate to be set as, most often, two  $\alpha$  particles were detected at forward angles and the proton was not. In order to set the proton gate simulated data for both break-up channels were used and Catania plots constructed. These 2D histograms are based on the rearranged  $Q$ -value equation,

$$E_b - E_t - E_1 - E_2 = \frac{p_p^2}{2} \frac{1}{m(p)} - Q, \quad (3)$$

where  $E_b$  is the beam energy,  $E_t$  the triton energy detected at the Q3D focal plane,  $E_{1,2}$  the energy of the two detected break-up particles in the DSSD array and  $p_p$  is the momentum of the reconstructed missing particle assumed to be a proton. The proton mass is  $m(p)$ . The resulting plots for the two decay channels are shown in Fig. 1.

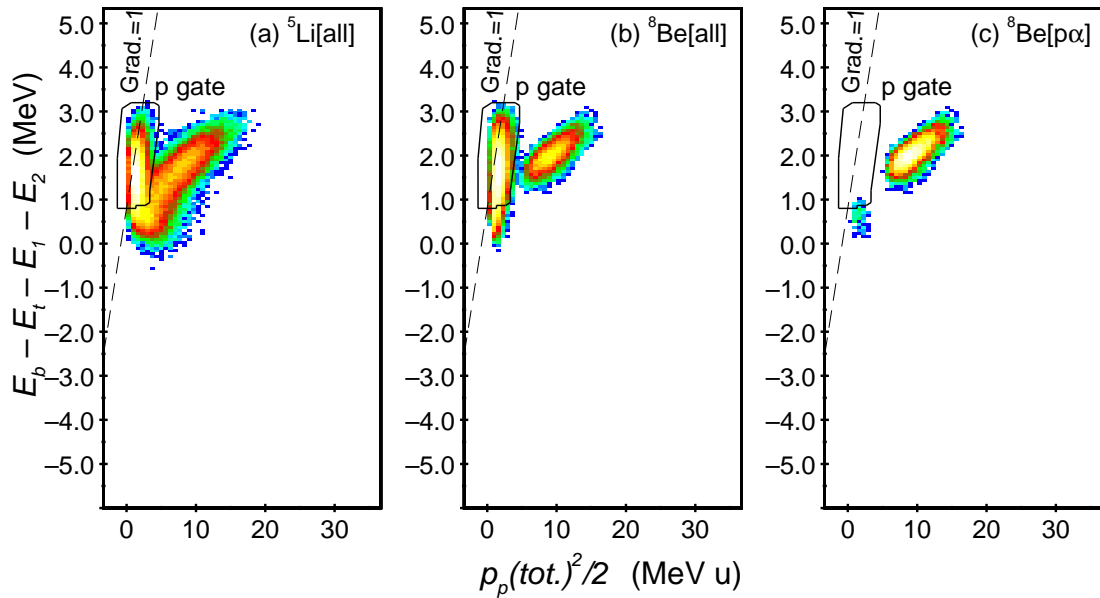


**Figure 1.** Catania plots for the simulated data for break-up channels (1) and (2) corresponding to the detection of two particles. See text for details. Panel (a):  ${}^5\text{Li}$  data with no requirement on which particles were detected. Panel (b): similarly for the  ${}^8\text{Be}$  break-up data. Panel (c): as for (b) but with the condition that detected particle (1) is a proton. The dashed line shows the gradient of the loci corresponding to  $1/m(p) = 1$ . The final proton gate used is shown with the continuous black outline. Note that the  $y$ -axis intercept at  $p_p/2 = 0$  is  $-Q$  (see Eqn. 3).

Figure 1 panels (a) and (b) show two clear distributions: corresponding, largely, to the missing particle being correctly identified as a proton (lying on the dashed lines) and to the missing particle being an  $\alpha$  particle (righthand distributions). However, there are some events, visible in Fig. 1 (c) for which detected-proton events lie close to the dashed line. The proton gate was therefore set to exclude such events. Though in Fig. 1 (c) a small fraction of these lie in the gate, this is the tail of the distribution and only visible due to the large number of simulated events,  $1 \times 10^6$  for each break-up channel. This is much larger than the number of events in the experimental data.

The results from the analysis are shown in Fig. 2(a). Here, the filtered data with all energy and particle cuts are shown, overlaid with a fit, using Voigt profiles [18] (continuous blue line).

A clear excess of counts can be seen at  $1.86 \text{ MeV} \pm 70 \text{ keV}(\text{stat}) \pm 35 \text{ keV}(\text{syst})$  with a width of  $650(160) \text{ MeV}$ . The overall  $\chi^2/d.o.f. = 1.13$ . The broad  $2.75 \text{ MeV}$  and narrow  $2.36 \text{ MeV}$  resonances are also required to fit the data.

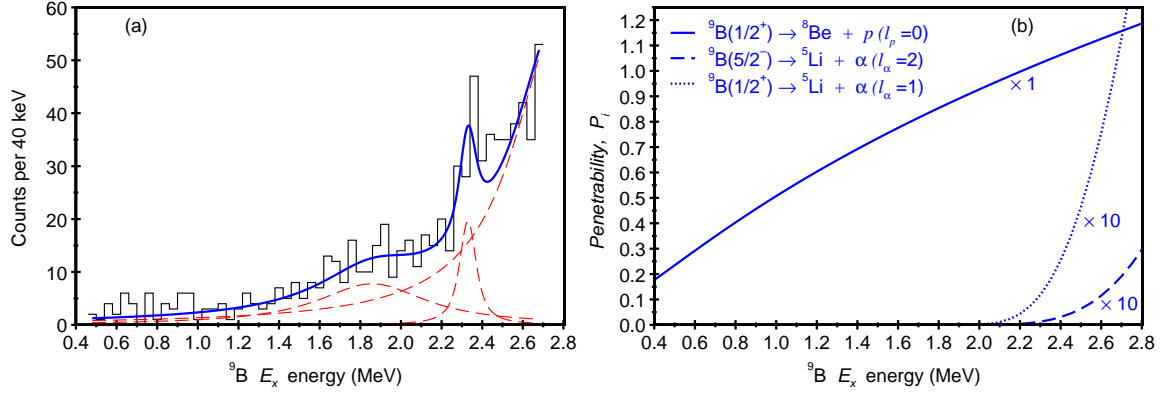


**Figure 2.** Panel (a): Data (black stepped line) with fit comprising three Voigt functions (continuous blue line) with fixed Gaussian width of  $41 \text{ keV}$  corresponding to the experimental resolution. The dashed red lines are the individual components: the known  $2.75$  and  $2.3 \text{ MeV}$  states along with a proposed state at  $1.86 \text{ MeV}$ . Modified from Fig. 6(a) of Ref. [8]. Panel (b): Penetrabilities (Eqn. 5) for the proton decay of a  $1/2^+$  state (continuous blue line), the  $\alpha$  decay of a  $5/2^-$  state (dashed blue line) such as the known  $2.3 \text{ MeV}$  state and the  $\alpha$  decay of a  $1/2^+$  state (dotted blue line). Note the different vertical scales. See text for details.

### 3. Decay penetrabilities

In order to compare the decay branches from resonances into different channels,  $i$ , the reduced width,  $\gamma_i^2$ , is used

$$\gamma_i^2 = \frac{\Gamma_i}{2P_i}, \quad (4)$$

with the barrier penetrabilities,  $P_i$ , removed. These can be written in terms of the wave number,  $k_i$ , radius,  $r_i$  ( $= 1.4(A_i^{1/3} + A_{recoil}^{1/3}) \text{ fm}$ ), and the regular,  $F_l(k_i r_i)$ , and irregular,  $G_l(k_i r_i)$ , Coulomb wave functions, such that

$$P_i = \frac{(k_i r_i)}{[F_l^2(k_i r_i) + G_l^2(k_i r_i)]}. \quad (5)$$

The penetrabilities for the two open decay channels below  $3 \text{ MeV}$  ( $p$  and  $\alpha$ ) are plotted in Fig. 2(b), calculated using the CKIN code [19] which utilises the CERN Libraries WCLBES code [20, 21]. As can be seen, the proton penetrabilities dominate up to  $2.8 \text{ MeV}$  which makes the decay-channel-filtering described earlier effective for the  $1/2^+$  state. Above the  $\alpha$ -decay threshold the  $\alpha$  penetrabilities increase rapidly, but even at  $2.0 \text{ MeV}$ , are orders of magnitude smaller than the corresponding proton values. However, beyond this, by  $2.3 \text{ MeV}$ , the  $5/2^-$  state overcomes the penetrabilities to decay  $99\%$  via  $\alpha$  emission [8, 9] – suggesting that this level has some  $\alpha$ -cluster structure – the  $\alpha$  preformation giving  $\alpha$  emission a preference over proton emission.

### 4. Summary

The coincidence method for ejectile-tagged break-up data for  ${}^9\text{B}$  has been elucidated for the case where two of the three break-up particles have been detected. Monte-Carlo simulations

have been used to obtain a selection window for events with an undetected proton, *i.e.* events with two detected  $\alpha$  particles. Following use of the proton gate, the  $^8\text{Be}$  ground-state has a significantly suppressed background from mis-identification of the particles and, when combined with other filtering criteria, almost background free  $^9\text{B}$  excitation spectra have been obtained. Finally, the penetrabilities for proton and  $\alpha$  decay up to 2.8 MeV in  $^9\text{B}$  have been calculated and plotted to demonstrate the applicability of the decay-channel selection technique.

## References

- [1] Tilley D R, Kelley J H, Godwin J L, Millener D J, Purcell J E, Sheua C G and Weller H R 2004 *Nucl. Phys. A* **745** 155
- [2] Thoennessen M. 2012 *At. Data Nucl. Data Tables* **98** 43
- [3] Haxby R O, Shoupp W E, Stephens W E, Wells W H 1940 *Phys. Rev.* **58** 1035
- [4] Baldwin T D, *et al.* 2012 *Phys. Rev. C* **86** 034330
- [5] Barker F C 2009 *Phys. Rev. C* **79** 017302
- [6] Fortune H T and Sherr R 2006 *Phys. Rev. C* **73** 064302
- [7] Arai K, Descouvemont P, Baye D and Catford W N 2003 *Phys. Rev. C* **68** 014310
- [8] Wheldon C, Kokalova Tz, *et al.* 2015 *Phys. Rev. C* **91** 024308
- [9] Gete E, *et al.* 2000 *Phys. Rev. C* **61** 064310
- [10] Löffler M, Scheerer H J and Vonach H 1973 *Nucl. Instr. and Meth.* **111** 1
- [11] Wirth H-F, Angerer H, von Egidy T, Eisermann Y, Graw G and Hertenberger R 2000 *Beschleunigerlaboratorium München, Annual Report* p71
- [12] Wirth H-F 2001 *Ph.D Thesis, Technical University, München*, see <http://tumb1.biblio.tu-muenchen.de/publ/diss/ph/2001/wirth.html>
- [13] Akimune H, Fujimura M, Fujiwara M, Hara K, Ishikawa T, Kawabata T, Utsunomiya H, Yamagata T, Yamasaki K and Yosoi M 2001 *Phys. Rev. C* **64** 041305(R)
- [14] Scholl C, *et al.* 2011 *Phys. Rev. C* **84** 014308
- [15] Curtis N, *et al.* 1995 *Phys. Rev. C* **51** 1554
- [16] Curtis N, *et al.* 1996 *Phys. Rev. C* **53** 1804
- [17] Tilley D R, Cheves C M, Godwin J L, Hale G M, Hofmann H M, Kelley J H, Sheu C G and Weller H R 2002 *Nucl. Phys. A* **708** 3
- [18] Gubner John A 1994 *J. Phys. A: Math Gen.* **27** L745
- [19] Wheldon C 2016 CKIN *Two-body kinematics code*, [http://www.np.ph.bham.ac.uk/research\\_resources/programs/](http://www.np.ph.bham.ac.uk/research_resources/programs/), accessed 01/10/2016
- [20] McLaren I 2006 *Wclbes.f subroutine*, [http://cernlib.sourcearchive.com/documentation/2006.dfsg.2/wclbes\\_8F\\_source.html](http://cernlib.sourcearchive.com/documentation/2006.dfsg.2/wclbes_8F_source.html), accessed 08/03/2016
- [21] Thompson I and Barnett A 1985 *Comput. Phys. Commun.* **36** 363